
NAVIC STANDARD SIMULATION Through Python

G. V. V. Sharma



Copyright ©2023 by G. V. V. Sharma.

<https://creativecommons.org/licenses/by-sa/3.0/>

and

<https://www.gnu.org/licenses/fdl-1.3.en.html>

Contents

| | | |
|------------|--|-----------|
| 1 | Introduction | 1 |
| 1.1 | Scope of simulation | 2 |
| 2 | NavIC System Overview | 3 |
| 2.1 | The Frequency Bands | 3 |
| 2.1.1 | L-band | 6 |
| 2.1.2 | S-band | 7 |
| 2.2 | NavIC Architecture | 8 |
| 2.2.1 | Space segment | 8 |
| 2.2.2 | Ground segment | 9 |
| 2.2.3 | User segment | 10 |
| 2.3 | NavIC Services | 11 |
| 2.3.1 | Standard Positioning Service (SPS) | 11 |
| 2.3.2 | Restricted Service (RS) | 11 |
| 3 | Transmitter | 12 |
| 3.1 | IRNSS Navigation data | 12 |
| 3.2 | Frame structure | 13 |

| | | |
|-------|---|----|
| 3.3 | Encoding | 14 |
| 3.3.1 | PRN codes for SPS | 14 |
| 3.3.2 | FEC Encoding | 16 |
| 3.3.3 | Interleaving | 17 |
| 3.3.4 | Sync word and Tail bits | 17 |
| 3.3.5 | Cyclic Redundancy Check(CRC) | 18 |
| 3.4 | Modulation | 18 |
| 3.4.1 | Standard Positioning Service | 18 |
| 3.4.2 | Baseband Modulation | 18 |
| 4 | Channel Modelling | 21 |
| 4.1 | Doppler shift | 21 |
| 4.2 | Delay | 23 |
| 4.3 | Power Scaling | 24 |
| 4.4 | Thermal noise | 25 |
| 5 | Receiver | 26 |
| 5.1 | Signal Acquisition | 28 |
| 5.1.1 | Implementation of CA PCPS Acquisition | 29 |
| 5.2 | Tracking | 31 |
| 5.2.1 | Carrier and code wipeoff | 31 |
| 5.2.2 | Pre-detection and integration | 33 |
| 5.2.3 | Baseband signal processing | 33 |

| | | |
|--------------|--|-----------|
| 5.3 | Demodulation | 38 |
| 5.4 | Decoding | 38 |
| 5.4.1 | Process | 39 |
| 5.4.2 | Convolutional Code Representation | 39 |
| 5.4.3 | Decoding Output | 41 |
| 5.4.4 | Example | 41 |
| 6 | Results | 44 |
| 6.1 | Acquisition | 44 |
| 6.2 | Tracking and Decoding | 45 |
| A | References | 47 |

List of Figures

| | | |
|-----|---|----|
| 2.1 | Frequency bands of NavIC Signals | 3 |
| 2.2 | NavIC Architecture | 9 |
| 2.3 | the NavIC bands segment blocks | 10 |
| 3.1 | Transmitter Block diagram | 12 |
| 3.2 | Master Frame Structure | 13 |
| 3.3 | Structure of subframe 1 and 2 | 14 |
| 3.4 | Structure of subframe 3 and 4 | 14 |
| 3.5 | SPS PRN Code Generator | 15 |
| 3.6 | FEC Encoding | 16 |
| 5.1 | The Block Level Architecture for Receiver | 27 |
| 5.2 | PCPS algorithm flow | 29 |
| 5.3 | Tracking block diagram | 32 |
| 5.4 | Generic baseband processor code and carrier tracking loops block diagram | 34 |
| 5.5 | The Block Level Architecture for Channel decoding | 39 |
| 5.6 | Trellis flow for Viterbi algorithm | 42 |

| | | |
|------------|---------------------------------------|-----------|
| 6.1 | Tracking result plot | 46 |
|------------|---------------------------------------|-----------|

List of Tables

| | | |
|------------|---|-----------|
| 2.2 | NavIC frequency bands | 3 |
| 3.2 | Code phase assignment for SPS signals | 16 |
| 3.4 | FEC encoding parameters | 17 |
| 3.6 | Symbol Description | 20 |
| 5.2 | Parameters Table in Signal Acquisition | 28 |
| 5.4 | Loop order filters | 37 |

Chapter 1

Introduction

NavIC (an acronym for 'Navigation with Indian Constellation') is the operational name for Indian Regional Navigation Satellite System (IRNSS), developed independently and indigenously by Indian Space Research Organization (ISRO). The objective of this autonomous regional satellite navigation system is to provide accurate real-time positioning and timing services to users in India and a region extending upto 1,500 km (930 mi) around it.

NavIC is designed with a constellation of 7 satellites and a network of ground stations operating 24 x 7. Three satellites of the constellation are placed in geostationary orbit and four satellites are placed in inclined geosynchronous orbit. The ground network consists of control centre, precise timing facility, range and integrity monitoring stations, two-way ranging stations, etc.

NavIC provides two levels of service, the "standard positioning service", which is open for civilian use, and a "restricted service" (an encrypted one) for authorised users (including the military). NavIC has a theoretical positional accuracy of 5m - 20m for general users and 0.5m for military purposes.

This book describes the NavIC standards simulation using Python code. Chapter 2 provides NavIC system overview, various frequency bands used and various services provided by NavIC. Chapter 3 describes the implementation details of Transmitter module. Chapter 4 details about various channeling parameters used in simulation. Chapter 5 elaborately describes the implementation details of Receiver module. Chapter 6 details out key results from the simulation.

1.1. Scope of simulation

The scope of the simulation is limited to

1. sending baseband signal (without a carrier) thorough transmitter module, mixing it with channel modelling module and verifying that the same baseband signal is received at the output of the receiver module.
2. baseband signals for L5 and S bands (L1 band is out of scope)
3. only SPS services signal (RS signal is out of scope)

Chapter 2

NavIC System Overview

2.1. The Frequency Bands

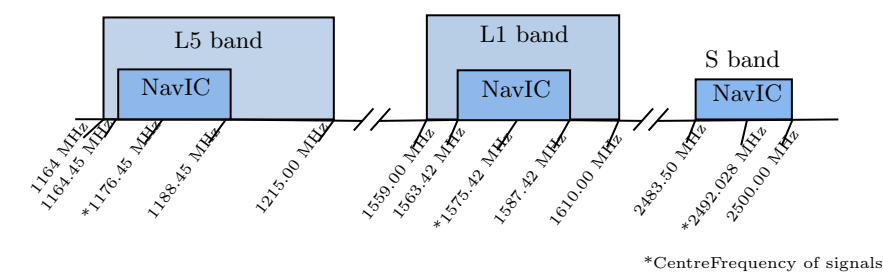


Figure 2.1: Frequency bands of NavIC Signals

| Bands | Carrier Frequency | Bandwidth | Usage |
|-------|-------------------|-----------|----------------------------|
| L1 | 1575.42 Mhz | 24 Mhz | for low power devices |
| L5 | 1176.45 Mhz | 24 Mhz | navigation and positioning |
| S | 2492.028 Mhz | 16.5 Mhz | SBAS and messaging |

Table 2.2: NavIC frequency bands

Satellite communication utilizes multiple frequency bands to accommodate different types of communication services and addresses various technical considerations. Here are some reasons why multiple frequency bands are used in satellite communication:

Spectrum Allocation: The electromagnetic spectrum is divided into various frequency bands to allocate different services and applications. This division ensures that different systems can operate without interfering with each other. By utilizing multiple frequency bands, satellite communication can effectively coexist with other wireless services and minimize interference issues.

Signal Propagation Characteristics: Different frequency bands exhibit unique propagation characteristics. Lower frequency bands, such as L band, have better signal penetration through obstacles and are less affected by atmospheric conditions, making them suitable for applications where signal reliability is crucial. Higher frequency bands, such as Ku band or Ka band, offer larger bandwidths and higher data transmission rates, making them ideal for applications requiring high-speed data transfer.

Bandwidth and Capacity: Different frequency bands offer varying bandwidths, and by utilizing multiple bands, satellite communication systems can increase overall capacity. This allows for the simultaneous transmission of multiple signals, accommodating a wide range of services such as television broadcasting, voice communication, internet access, and data transfer.

Frequency Reuse and Interference Mitigation: Satellite systems employ frequency reuse techniques to maximize the utilization of the available frequency spectrum. By using different frequency bands, satellite operators

can reuse frequencies in different geographical areas without causing interference. This allows for efficient utilization of the limited spectrum resources.

Regulation and International Coordination: The allocation and usage of frequency bands are regulated by international bodies and national spectrum management organizations. These regulations help ensure efficient spectrum utilization, prevent interference between different systems, and promote global coordination and compatibility of satellite communication services.

In summary, the use of multiple frequency bands in satellite communication enables efficient spectrum utilization, accommodates different services, and addresses various technical considerations such as signal propagation, bandwidth, capacity, and interference mitigation. By leveraging the advantages offered by different frequency ranges, satellite systems can provide reliable, high-speed communication services to a wide range of applications and users.

The seven satellites in the NavIC constellation so far use two frequencies for providing positioning data — the L5 and S bands. This was because India hadn't received the International Telecommunication Union authorisation for using the L1 and L2 frequency bands, which are widely used worldwide for navigation services. The new satellites NVS-01 onwards, meant to replace these satellites, will also have L1 band. L1 is an interoperable frequency and can be used across all chipsets(of mobile devices), provided they use our signal architecture.

2.1.1. L-band

The L band offers several advantages for wireless communication systems, including a balance between signal propagation characteristics and antenna size. It provides good signal penetration through various atmospheric conditions, vegetation, and even some obstacles. These properties make it suitable for applications such as satellite communication, navigation systems, and mobile networks.

Satellite communication is one of the significant applications of the L band. Satellites in geostationary orbits often utilize this frequency range for broadcasting television signals, as well as for maritime, navigation and aeronautical communications. The L band allows for reliable and efficient transmission over long distances, making it a valuable resource for global connectivity. Because of satellites' increased use, number and size, congestion has become a serious issue in the lower frequency bands.

L1 and L5 are specific frequencies within the L band that are used in Global Navigation Satellite Systems (GNSS), such as GPS (Global Positioning System), NavIC and Galileo. These frequencies play a crucial role in providing accurate positioning, navigation, and timing information.

2.1.1.1. L1

L1 refers to the first frequency within the L band used by GNSS. In NavIC, the L1 frequency is centered around 1575.42 MHz. The L1 signal carries the primary navigation message and is used for standard positioning and timing applications. It is widely used in various sectors, including transportation,

surveying, and consumer applications like personal navigation devices and smartphones.

2.1.1.2. L5

L5, on the other hand, is an additional frequency introduced in modernized GNSS systems like GPS and Galileo. In NavIC, the L5 frequency is centered around 1176.45 MHz. It was introduced to provide improved accuracy, integrity, and resistance to interference. The L5 signal carries more precise and reliable positioning information, making it particularly useful in critical applications that require high levels of accuracy, such as aviation, surveying, and scientific research. The L1 frequency offers broad coverage and compatibility with legacy systems, while the L5 frequency provides more precise positioning and improved resistance to interference. The combination of these frequencies allows for more reliable and accurate navigation solutions, benefiting a wide range of industries and applications.

2.1.2. S-band

The S band is another frequency range within the electromagnetic spectrum, located between the L band and the C band. It spans a frequency range of approximately 2 to 4 GHz. In NavIC, S band frequency is centred around 2492.028 MHz. The S band finds applications in various fields, including communication, radar systems, satellite broadcasting, and scientific research.

One of the primary uses of the S band is in satellite communication. Satel-

lites in geostationary orbits often utilize S band frequencies for uplink and downlink communication with ground stations. The S band provides a good balance between antenna size and data capacity, making it suitable for broadcasting television signals, voice communication, and data transmission. However, the higher frequency bands typically give access to wider bandwidths, but are also more susceptible to signal degradation due to ‘rain fade’ (the absorption of radio signals by atmospheric rain, snow or ice).

2.2. NavIC Architecture

The NavIC architecture is as shown in Fig 2.2. It mainly consists of

1. Space segment
2. Ground segment
3. User segment

2.2.1. Space segment

Space segment consists of a constellation of 7 satellites. Three satellites of the constellation are placed in geostationary orbit, at 32.5°E , 83°E and 129.5°E respectively, and four satellites are placed in inclined geosynchronous orbit with equatorial crossing of 55°E and 111.75°E respectively, with inclination of 29° (two satellites in each plane).

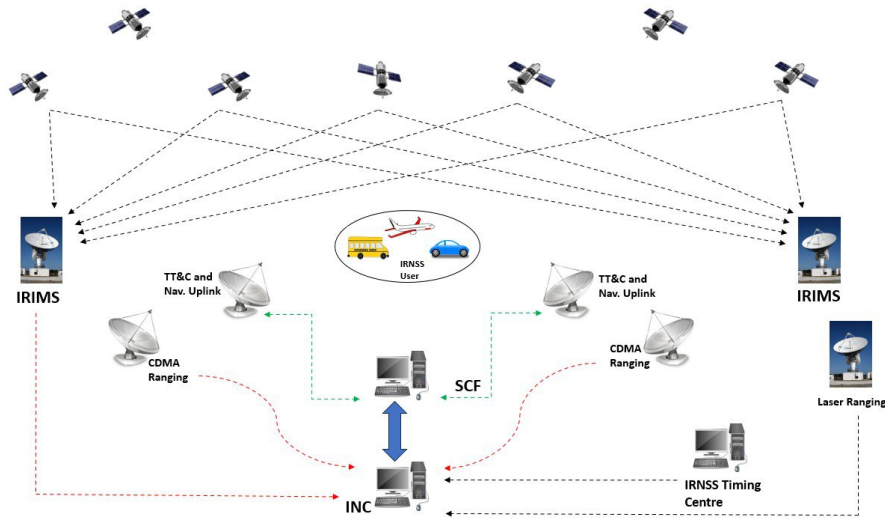


Figure 2.2: NavIC Architecture

2.2.2. Ground segment

Ground segment takes care of operation and maintenance of the constellation. It consists of

1. ISRO Navigation Centre
2. IRNSS Spacecraft Control Facility
3. IRNSS Range and Integrity Monitoring Stations
4. IRNSS Network Timing Centre
5. IRNSS CDMA Ranging Stations
6. Laser Ranging Stations
7. Data Communication Network

2.2.3. User segment

User segment consists of

1. A single frequency receiver having capability to receive SPS signal at either L1, L5 or S band frequency
2. A multi-frequency receiver having capability to receive SPS signal at combination of L1, L5 and S band frequencies
3. A multi-constellation receiver compatible with NavIC and other GNSS signals.

The Figure2.3 above specifies the radio frequency interface between space and user segments.

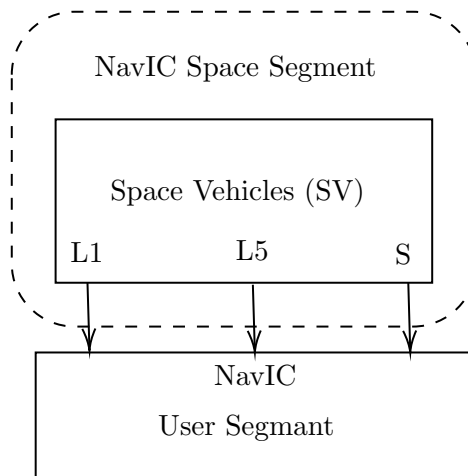


Figure 2.3: the NavIC bands segment blocks

2.3. NavIC Services

The NavIC provides basically two types of services:

1. Standard Positioning Service (SPS)
2. Restricted Service (RS)

Both SPS and RS signals contain ranging codes that allow receivers to compute their travelling time from satellite to receiver, along with navigation data, in order to know the satellite's position at any time.

2.3.1. Standard Positioning Service (SPS)

It is available to all civilian users free of charge and provides positioning, navigation, and timing information with a moderate level of accuracy. The SPS signals in NavIC primarily operate in the L5 and S frequency bands.

2.3.2. Restricted Service (RS)

The RS is intended for authorized users and offers enhanced accuracy, integrity, and availability compared to the SPS signals. The RS signals in NavIC operate in both the L5 and S bands and broadcast through a phased array antenna to keep required coverage and signal strength.

Chapter 3

Transmitter

The NavIC transmitter is simulated to send baseband signal to the channel as shown in Fig 3.1.

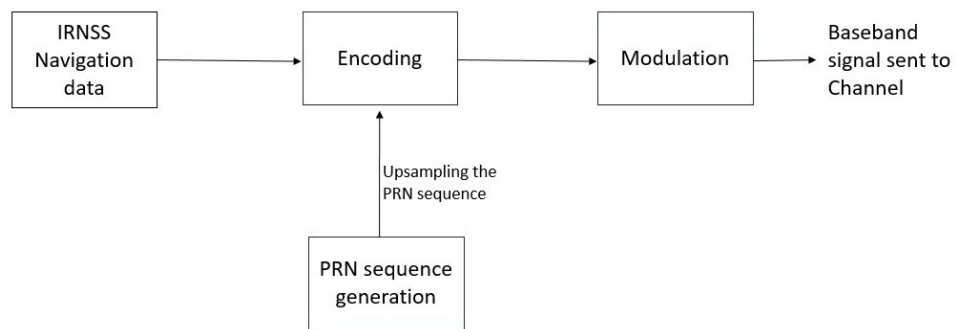


Figure 3.1: Transmitter Block diagram

3.1. IRNSS Navigation data

Navigation data in satellite communication refers to the crucial information transmitted between satellites and ground-based receivers to facilitate accurate positioning and navigation. It includes data related to satellite orbits, precise timing, and other parameters necessary for determining the satellite's

position relative to the Earth's surface.

3.2. Frame structure

NavIC master frame consists of 2400 symbols, divided into 4 subframes. Each subframe is 600 symbols long. Each subframe has 16 bit Sync word followed by 584 bits of interleaved data. Subframes 1 and 2 transmit fixed primary navigation parameters. Subframe 3 and 4 transmit secondary navigation parameters in the form of messages. The master frame structure is shown in figure 3.2.

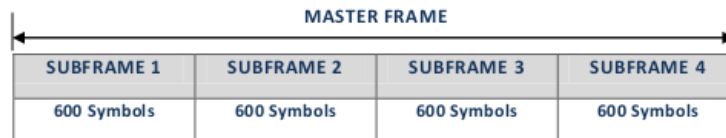


Figure 3.2: Master Frame Structure

Each subframe is 292 bits long without FEC encoding and sync word. It starts with TLM word of 8 bits and ends with 24 bit Cyclic Redundancy Check(CRC) followed by 6 tail bits. In subframes 1 and 2 navigation data is allotted with 232 bits, starting from bit 31. In subframe 3 and 4, 220 bits are allotted starting from bit 37. The typical structure of the subframes are shown in figure 3.3 and figure 3.4 respectively.

| | | | | | | | | | |
|--------|--------|-------|---------|-------------|-------|----|----------|--------|-------|
| 1 | 9 | 26 | 27 | 28 | 30 | 31 | | 263 | 287 |
| TLM | TOWC | ALERT | AUTONAV | SUBFRAME ID | SPARE | | DATA | CRC | Tail |
| 8 BITS | 17BITS | 1 BIT | 1 BIT | 2 BIT | 1 BIT | | 232 BITS | 24BITS | 6BITS |

Figure 3.3: Structure of subframe 1 and 2

| | | | | | | | | | | |
|--------|--------|-------|---------|-------------|-------|------------|----------|--------|---------|--------|
| 1 | 9 | 26 | 27 | 28 | 30 | 31 | 37 | 257 | 263 | 287 |
| TLM | TOWC | ALERT | AUTONAV | SUBFRAME ID | SPARE | MESSAGE ID | DATA | PRN ID | CRC | Tail |
| 8 BITS | 17BITS | 1 BIT | 1 BIT | 2 BIT | 1 BIT | 6 BITS | 220 BITS | 6 | 24 BITS | 6 BITS |

Figure 3.4: Structure of subframe 3 and 4

3.3. Encoding

3.3.1. PRN codes for SPS

PRN Codes selected for Standard Positioning System are similar to GPS C/A Gold codes. The length of each code is 1023 chips. The code is chipped at 1.023 Mcps.

For SPS code generation, the two polynomials G1 and G2 are as defined below:

$$G1 : X^{10} + X^3 + 1 \quad (3.1)$$

$$G2 : X^{10} + X^9 + X^8 + X^6 + X^3 + X^2 + 1 \quad (3.2)$$

Polynomial G1 and G2 are similar to the ones used by GPS C/A signal. The G1 and G2 generators are realized by using 10 bits Maximum Length

Feedback Shift Registers(MLFSR). The initial state of G2 provides the chip delay. The G1 register is initialized with all bits as 1. G1 and G2 are XOR'ed for the generation of the final 1023 chip long PRN sequence. The SPS PRN code generator is shown in figure 3.5.

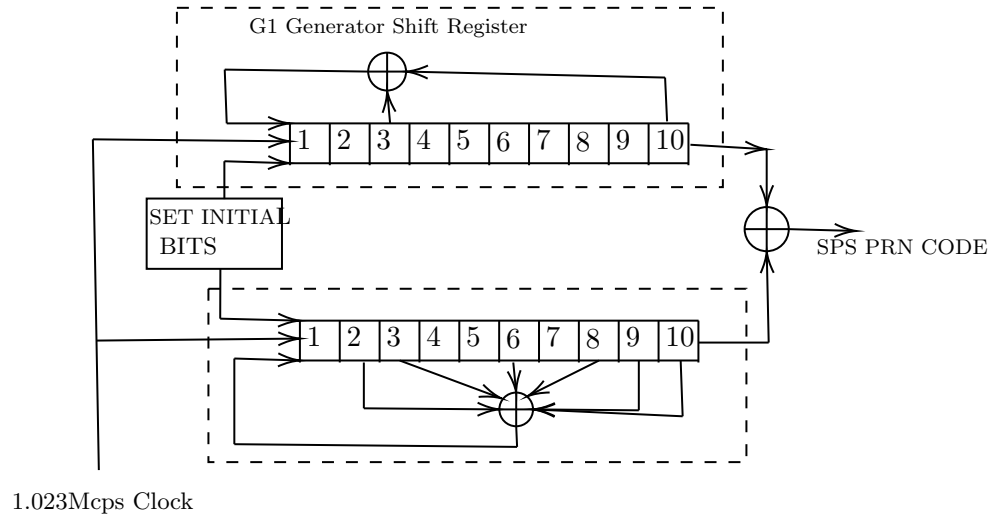


Figure 3.5: SPS PRN Code Generator

The satellites that are used in the current simulation are with PRN ids - 1, 3, 5 and 7. The initial condition of G2 register in L5 and S bands for the given PRN ids is given in table 3.2.

| PRN ID | L5-SPS G2 initial condition | S-SPS G2 initial condition |
|-----------|--------------------------------|-------------------------------|
| 1 | 1110100111 | 0011101111 |
| 3 | 1000110100 | 1000110001 |
| 5 | 1110110000 | 1010010001 |
| 7 | 0000010100 | 0010001110 |

Table 3.2: Code phase assignment for SPS signals

3.3.2. FEC Encoding

The Navigation data subframe of 292 bits is convolution encoded with a rate of 1/2 and clocked at 50 symbols per second. The coding scheme is given in figure 3.6. Each subframe of 292 bits, after encoding, results in 584 symbols. Various FEC encoding parameters used in NavIC are tabulated in table 3.4.

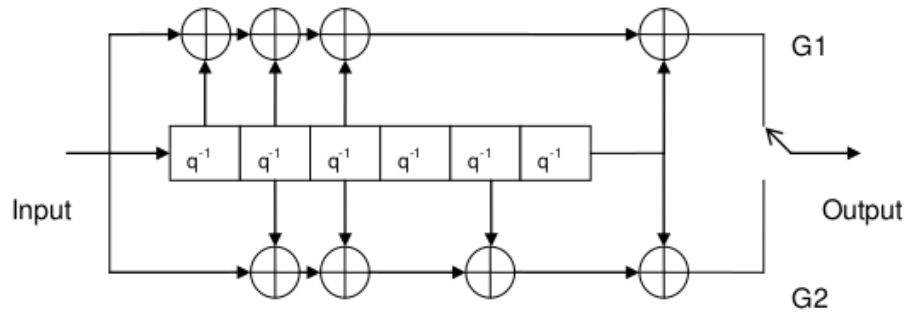


Figure 3.6: FEC Encoding

| Parameter | Value |
|----------------------|--|
| Coding Rate | $\frac{1}{2}$ |
| Coding Scheme | Convolution |
| Constraint Length | 7 |
| Generator Polynomial | G1=(171) _o G2=(133) _o |
| Encoding Sequence | G1 then G2 |

Table 3.4: FEC encoding parameters

3.3.3. Interleaving

Any burst errors during the data transmission can be corrected by interleaving. In matrix interleaving, input symbols are filled into a matrix column wise and read at the output row wise. This will spread the burst error, if any, during the transmission. For SPS, data is filled into matrix of size 73 by 8(73 columns, 8 rows).

3.3.4. Sync word and Tail bits

Each subframe has a 16 bit word synchronization pattern which is not encoded. Sync pattern is *EB90* Hex. Tail bits consist of 6 zero value bits added to the subframe and tail bits are part of FEC encoding.

3.3.5. Cyclic Redundancy Check(CRC)

The parity coding of data signal follows 24Q polynomial for each subframe. 24 bits of CRC parity will provide protection against burst as well as random errors with undetected error probability of 2^{-24} for all channel bit error probabilities 0.5.

$$g(X) = \sum_{i=0}^{24} g_i X^i \quad (3.3)$$

$$g_i = 1; \text{ for } i = 0, 1, 3, 4, 5, 6, 7, 10, 11, 14, 17, 18, 23, 24$$
$$= 0 \text{ otherwise}$$

3.4. Modulation

3.4.1. Standard Positioning Service

The SPS signal is BPSK(1) modulated on L5 and S bands. The navigation data at data rate of 50 sps (1/2 rate FEC encoded) is modulo 2 added to PRN code chipped at 1.023 Mcps. The CDMA modulated code is up-converted by the L5 and S carriers at 1176.45 MHz and 2492.028 MHz respectively. However, this simulation does not carry out this upconversion.

3.4.2. Baseband Modulation

The carrier signal is modulated by BPSK(1), Data channel BOC(5,2), and Pilot Channel BOC(5,2). To have a constant envelop when passed through power amplifier, we add additional signal called interplex signal.

3.4.2.1. Mathematical Equations

The following equations describe baseband signals for L5 and S band navigation data.

SPS Data Signal:

$$s_{sps}(t) = \sum_{i=-\infty}^{\infty} c_{sps}(|i|_{L_sps}).d_{sps}([i]_{CD_sps}).\text{rect}_{T_{c,sps}}(t - iT_{c,sps}) \quad (3.4)$$

RS BOC Pilot Signal:

$$s_{rs-p}(t) = \sum_{i=-\infty}^{\infty} c_{rs-p}(|i|_{L_rs-p}).\text{rect}_{T_{c,rs-p}}(t - iT_{c,rs-p}).sc_{rs-p}(t, 0) \quad (3.5)$$

RS BOC Signal:

$$s_{rs-d}(t) = \sum_{i=-\infty}^{\infty} c_{rs-d}(|i|_{L_rs-d}).d_{rs-d}([i]_{CD_rs-d}).\text{rect}_{T_{c,rs-d}}(t - iT_{c,rs-d}).sc_{rs-d}(t, 0) \quad (3.6)$$

The sub-carrier is defined as:

$$sc_x(t, \phi) = \text{sgn} [\sin(2\pi f_{sc,x}t + \phi)] \quad (3.7)$$

The IRNSS RS data and pilot BOC signals are sinBOC. Hence the subcarrier phase $\phi = 0$. The complex envelope of composite signal with Interplex signal (I(t)) is:

$$s(t) = \frac{1}{3} \left[\sqrt{2}(s_{sps}(t) + s_{rs-p}(t)) + j(2.s_{rs-d}(t) - I(t)) \right] \quad (3.8)$$

The Interplex signal $I(t)$ is generated to realize the constant envelope composite signal. The operation $|i|_X$ gives the code chip index for any signal. Similarly $[i]_X$ gives data bit index for any signal. Symbol definitions are given in below table 3.6.

| Symbol | Definition |
|-----------|------------------------------------|
| A | received signal amplitude |
| f_c | carrier frequency |
| f_{sub} | subcarrier frequency |
| t | time |
| q | phase offset |
| s(t) | BPSK signal transmitted data(-1,1) |

Table 3.6: Symbol Description

The functions for data generation, SPS-PRN sequence generation and baseband modulation are present in the below code.

```
codes/transmitter/transmitter.py
```

Chapter 4

Channel Modelling

The phenomena modelled in the satellite communication channel are

1. Doppler shift
2. Delay
3. Power scaling and
4. Thermal noise at the receiver

4.1. Doppler shift

Due to relative motion between the satellites and the receiver, the transmitted signals undergo a frequency shift before arriving at the receiver. This shift in frequency is called Doppler shift and can be computed as

$$f_{shift} = f_d - f_c = \left(\frac{V_{rel}}{c - V_{S,dir}} \right) f_c \quad (4.1)$$

where,

f_{shift} = Frequency shift due to Doppler effect

f_d = Frequency observed at receiver

f_c = Carrier frequency at transmitter

V_{rel} = Relative velocity of transmitter and receiver

$V_{S,dir}$ = Velocity of satellite along radial direction

c = Speed of light

V_{rel} is given by

$$V_{rel} = V_{S,dir} - V_{R,dir} \quad (4.2)$$

where,

$V_{R,dir}$ = Velocity of receiver along radial direction

$V_{R,dir}$ and $V_{S,dir}$ are given by

$$V_{R,dir} = \mathbf{V}_R \cdot \hat{\mathbf{d}}\mathbf{r} \quad (4.3)$$

$$V_{D,dir} = \mathbf{V}_S \cdot \hat{\mathbf{d}}\mathbf{r} \quad (4.4)$$

where,

$\hat{\mathbf{d}}\mathbf{r}$ = Unit vector from satellite to receiver i.e. radial direction

\mathbf{V}_S = Velocity of satellite

\mathbf{V}_R = Velocity of receiver

$\hat{\mathbf{d}}\mathbf{r}$ is given by

$$\hat{\mathbf{d}}\mathbf{r} = \frac{\mathbf{P}_S - \mathbf{P}_R}{\|\mathbf{P}_S - \mathbf{P}_R\|} \quad (4.5)$$

where,

$\mathbf{P_S}$ = Position of satellite

$\mathbf{P_R}$ = Position of receiver

The Doppler shift is introduced by multiplying the satellite signal with a complex exponential,

$$x_{Shift}[n] = x[n] e^{-2\pi j(f_c + f_{Shift})nt_s} \quad (4.6)$$

where,

$x_{Shift}[n]$ = Doppler shifted signal

$x[n]$ = Satellite signal

t_s = Sampling period

4.2. Delay

Since there is a finite distance between the satellite and the receiver, the signal at the receiver is a delayed version of the transmitted signal. This delay is given by

$$D_s = \frac{d}{c} f_s \quad (4.7)$$

where,

D_s = Total delay in samples

d = Distance between satellite and receiver

c = Speed of light

f_s = Sampling rate

The total delay on the satellite signal is modeled in two steps. First, a

static delay is modeled which does not change with time and it is always an integer number of samples. Then, a variable delay is modeled which can be a rational number of samples. While modelling the static delay, the entire delay is not introduced so that variable delay modelling handles the remaining delay.

To introduce the static delay, the samples are read from a queue whose size is the desired static delay length. When samples are read from the queue, an equal number of new samples are updated in the queue. To introduce the variable delay, the signal is passed through an all-pass FIR filter with an almost constant phase response. Its coefficients are calculated using the delay value required.

4.3. Power Scaling

When a transmitting antenna transmits radio waves to a receiving antenna, the radio wave power received is given by,

$$P_r = P_t D_t D_r \left(\frac{1}{4\pi (f_c + f_{Shift}) D} \right)^2 \quad (4.8)$$

where,

P_r = Received power

P_t = Transmitted power

D_t = Directivity of transmitting antenna

D_r = Directivity of receiving antenna

D = Total delay in seconds

To scale the received signal as per the received power calculated,

$$x_{Scaled}[n] = \frac{\sqrt{P_r}}{\text{rms}(x[n])} x[n] \quad (4.9)$$

4.4. Thermal noise

The thermal noise power at the receiver is given by,

$$N_r = kTB \quad (4.10)$$

where,

N_r = Noise power in watts

k = Boltzmann's constant

T = Temperature in Kelvin

B = Bandwidth in Hz

AWGN (Additive White Gaussian Noise) samples with zero mean and variance N_r are generated and added to the satellite signal to model thermal noise at receiver.

The functions necessary to model the channel are present in the below code,

`codes/channelmodel/channelmodel.py`

Chapter 5

Receiver

The signal processing chain at the receiver are divided into four steps:

1. Signal acquisition
2. Signal tracking
 - (a) Carrier Tracking
 - (b) Code Tracking
3. Signal demodulation
4. Channel decoding

The signal processing part for NavIC signals at receiver are as shown in figure 5.1.

1. **Signal acquisition:** The receiver searches for and acquires the NavIC signal for a given satellite(s) by correlating the received signal with a locally generated replica of the spreading code used by the satellite(s).

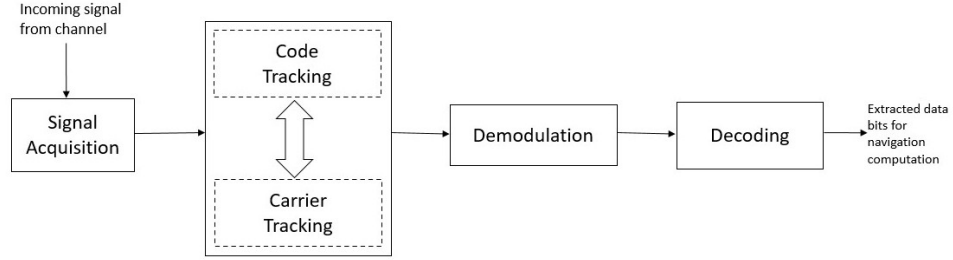


Figure 5.1: The Block Level Architecture for Receiver

This process helps in identifying the presence of the NavIC signal and estimating coarse value of both doppler frequency shift and code delay.

2. **Carrier tracking:** Once the signal is acquired, the receiver performs carrier tracking to estimate and track the carrier frequency and phase of the received signal. This is crucial for demodulation as it ensures accurate demodulation of the navigation message and ranging signal.
3. **Code delay tracking:** The receiver performs code delay tracking to estimate and track the spreading code used by the satellites. This helps in maintaining synchronization with the transmitted signal and extracting the navigation data and ranging information.
4. **Signal demodulation:** After the acquisition and tracking has been performed, the received data is mapped back using BPSK demodulation, mapping -1 to binary 1 and $+1$ to binary 0.
5. **Signal decoding:** Once the signal has been demodulated, the decoding is performed removing all the extra bits that were added to navigation data during the encoding process.

5.1. Signal Acquisition

The role of the acquisition block is to examine the presence/absence of signals coming from a given satellite. In the case of signal being present, it should provide coarse estimations of the Code delay and the Carrier Doppler shift, yet accurate enough to initialize the frequency and code tracking loops.

A generic IRNSS signal defined by its complex baseband equivalent, $S_T(t)$, the digital signal at the input of an Acquisition block can be written as:

$$x_{IN}[k] = A(t)\hat{s}_T(t - \tau(t))e^{j(2\pi f_D(t)t + \Phi(t))} \Big|_{t=kT_s} + n(t) \Big|_{t=kT_s} \quad (5.1)$$

| Symbol | Definition |
|----------------|--|
| $x_{IN}[k]$ | Complex vector I, Q samples of received signal |
| $A(t)$ | Signal Amplitude |
| $\hat{s}_T(t)$ | filtered version of $s_T(t)$ |
| $f_D(t)$ | Time varying doppler shift |
| $\Phi(t)$ | Time varying carrier phase shift |
| $\tau(t)$ | Time varying code delay |
| $n(t)$ | Time varying random noise |
| T_s | Sampling period |

Table 5.2: Parameters Table in Signal Acquisition

5.1.1. Implementation of CA PCPS Acquisition

The Parallel Code Phase Search (PCPS) algorithm is used in Acquisition block and is depicted in figure 5.2 and described as follows:

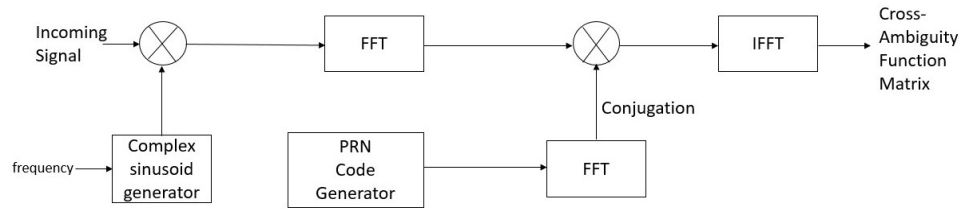


Figure 5.2: PCPS algorithm flow

Given:

1. Input signal buffer x_{IN} of K complex samples, provided by the Signal Conditioner
2. On-memory FFT of the local replica

$$D[k] = FFT_K\{d[k]\} \quad (5.2)$$

3. Acquisition threshold γ
4. Frequency span : $[f_{min}, f_{max}]$
5. Frequency step : f_{step}

Expected:

1. Find out if signal is acquired or not for a given satellite(s)

2. If signal is acquired, for each given satellite, calculate coarse estimation of Doppler shift $\hat{f}_{D_{acq}}$ and Code delay $\hat{\tau}_{acq}$

Algorithm:

1. Calculate input signal power estimation $\hat{P}_{in} = \frac{1}{K} \sum_{k=0}^{K-1} |x_{IN}[k]|^2$
2. for $\check{f}_D = [f_{min} to f_{max}]$ in f_{steps}
 - (a) Calculate carrier wipe off $x[k] = x_{IN}[k]e^{-(j2\pi\check{f}_D k T_s)}$, for $k = 0, \dots, K-1$
 - (b) Calculate $X[k] = FFT_K\{x[k]\}$
 - (c) Calculate $Y[k] = X[k].D[k]$, for $k = 0, \dots, K-1$
 - (d) Calculate corresponding column in the Cross ambiguity function matrix - $R_{xd}(\check{f}_D, \tau) = \frac{1}{K^2} IFFT_K\{Y[k]\}$
3. Search maximum and its indices in the search grid:

$$\{S_{max}, f_i, \tau_j\} = \max_{f, \tau} |R_{xd}(f, \tau)|^2 \quad (5.3)$$

4. Calculate the Generalized Likelihood Ratio Test (GLRT) function with normalized variance:

$$\Gamma_{GLRT} = \frac{2KS_{max}}{\hat{P}_{in}} \quad (5.4)$$

5. if $\Gamma_{GLRT} > \gamma$

Declare positive acquisition and provides coarse estimation of code delay $\hat{\tau}_{acq} = \tau_j$ and Doppler shift $\hat{f}_{D_{acq}} = f_i$,

other wise declare negative acquisition.

The acquisition results are generated using the below code

Code

```
code/e2e_sim/main.ipynb
```

5.2. Tracking

The role of tracking block is to follow signal synchronization parameters: code phase, Doppler shift and carrier phase and extract the baseband signal. It performs the following 3 function to decipher the baseband signal from the incoming signal as shown in figure 5.3.

1. Carrier and code wipeoff
2. Pre-detection integration
3. Baseband signal processing

5.2.1. Carrier and code wipeoff

Carrier wipeoff: Referring to the figure 5.3, first the digital IF is stripped off the carrier (plus carrier Doppler) by the replica carrier (plus carrier Doppler) signals to produce in-phase (I) and quadrature (Q) sampled data. The I and Q signals at the outputs of the mixers have the desired phase

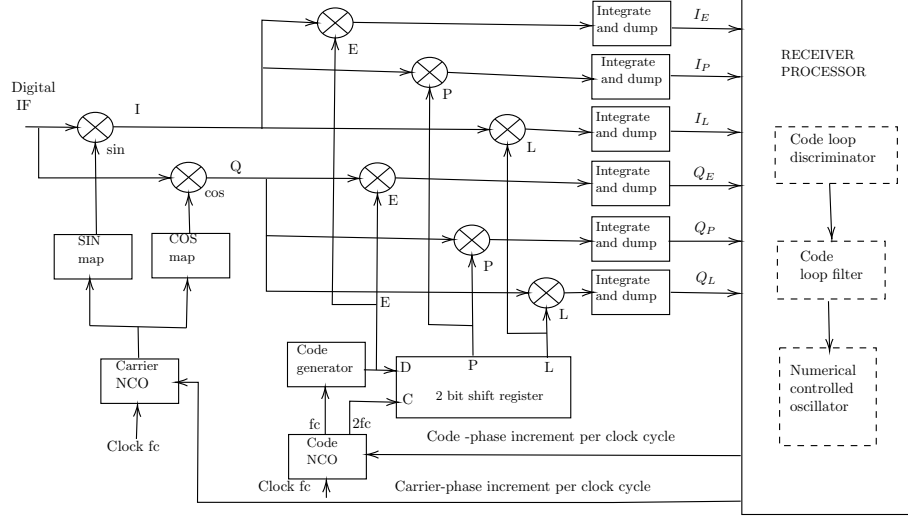


Figure 5.3: Tracking block diagram

relationships with respect to the detected carrier of the desired satellite. The replica carrier (including carrier Doppler) signals are synthesized by the carrier numerically controlled oscillator (NCO) and the discrete sine and cosine mapping functions. In closed loop operation, the carrier NCO is controlled by the carrier tracking loop in the receiver processor.

Code wipeoff: The I and Q signals are then correlated with early(E), prompt(P), and late(L) replica codes (plus code Doppler) synthesized by the code generator, a 2-bit shift register, and the code NCO. In closed loop operation, the code NCO is controlled by the code tracking loop in the receiver processor. E and L are typically separated in phase by 1 chip and P is in the middle. The prompt replica code phase is aligned with the incoming satellite code phase producing maximum correlation if it is tracking the incoming satellite code phase. Under this circumstance, the early phase is

aligned a fraction of a chip period early, and the late phase is aligned the same fraction of the chip period late with respect to the incoming code phase, and these correlators produce about half the maximum correlation. Any misalignment in the replica code phase with respect to the incoming code phase produces a difference in the vector magnitudes of the early and late correlated outputs so that the amount and direction of the phase change can be detected and corrected by the code tracking loop.

5.2.2. Pre-detection and integration

Extensive digital predetection integration and dump processes occur after the carrier and code wiping off processes. Figure 5.3 shows three complex correlators required to produce three in-phase components, which are integrated and dumped to produce I_E, I_P, I_L and three quadrature components integrated and dumped to produce Q_E, Q_P, Q_L . The carrier wipeoff and code wipeoff processes must be performed at the digital IF sample rate, while the integrate and dump accumulators provide filtering and resampling at the processor baseband input rate, which can be at 1,000 Hz during search modes or as low as 50 Hz during track modes, depending on the desired dwell time during search or the desired predetection integration time during track.

5.2.3. Baseband signal processing

This entails Carrier tracking and Code tracking using Phase locked loop (PLL), Frequency locked loop (FLL) and Delay locked loop (DLL). The

general block diagram is as shown in Figure 5.4.

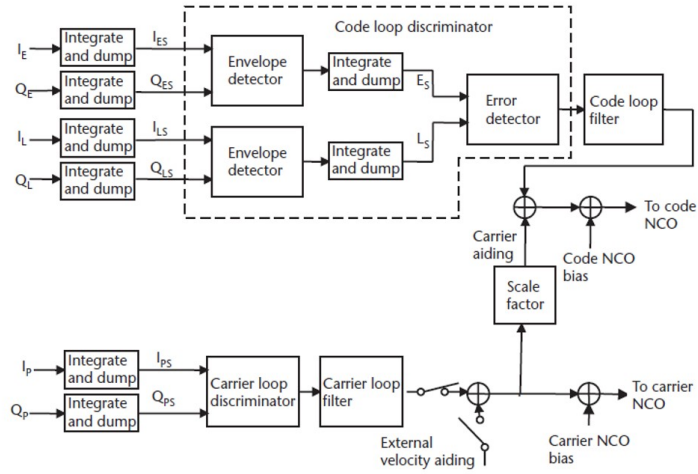


Figure 5.4: Generic baseband processor code and carrier tracking loops block diagram

5.2.3.1. Carrier tracking loop

Phase locked loop(PLL)

The carrier loop discriminator defines the type of tracking loop as a PLL, a Costas PLL (which is a PLL-type discriminator that tolerates the presence of data modulation on the baseband signal), or a frequency lock loop (FLL). Carrier tracking loop tracks the frequency and phase of the received signal by detecting the phase error between replicated signal and incoming signal and accordingly replicated signal produced by numerically controlled oscillator (NCO) is adjusted to synchronize with incoming signal in both frequency and

phase. For zero phase error detected, navigation data is accurately extracted.

$$\text{Phase error} = \text{ATAN2}(I_P, Q_P) = \tan^{-1} \left(\frac{I_P}{Q_P} \right) \quad (5.5)$$

The ATAN2 discriminator is the only one that remains linear over the full input error range of $\pm 180^\circ$. However, in the presence of noise, both of the discriminator outputs are linear only near the 0° region. These PLL discriminators will achieve the 6-dB improvement in signal tracking threshold (by comparison with the Costas discriminators) for the dataless carrier because they track the full four quadrant range of the input signal.

Frequency locked loop

PLLs replicate the exact phase and frequency of the incoming SV (converted to IF) to perform the carrier wipeoff function. FLLs perform the carrier wipeoff process by replicating the approximate frequency, and they typically permit the phase to rotate with respect to the incoming carrier signal. The algorithm used in FLL discriminator is $\frac{\text{ATAN2}(\text{cross}, \text{dot})}{t_2 - t_1}$. The frequency error is given by

$$\text{Frequency error} = \frac{\phi_2 - \phi_1}{t_2 - t_1} \quad (5.6)$$

The pahse change $\phi_2 - \phi_1$ between two adjacent samples of I_{PS} and Q_{PS} at times t_2 and t_1 is computed. This phase change in a fixed interval of time is proportinal to frequenct error in the carrier tracking loop. The error is fed to carier NCO to adjust the frequency to lock to the right frequency.

5.2.3.2. Code tracking loop

Delay locked loop: Post the carrier signal synchronization, received CA code samples are synchronized by aligning with replicated CA code samples by shifting right or left. To determine the direction of shift, the I and Q outputs are multiplied with prompt code (PRN code which is phase aligned), early code (prompt PRN code shifted by some samples to the right) and late code (prompt PRN code shifted by some samples to the left) resulting in corresponding to I and Q channel respectively. Following algorithm is used to lock the code phase.

$$E = \sqrt{I_{ES}^2 + Q_{ES}^2} \quad (5.7)$$

$$L = \sqrt{I_{LS}^2 + Q_{LS}^2} \quad (5.8)$$

$$\text{DLL Discriminator}(\epsilon) = \frac{1}{2} \frac{E - L}{E + L} \quad (5.9)$$

If the replica code is aligned, then the early and late envelopes are equal in amplitude and no error is generated by the discriminator. If the replica code is misaligned, then the early and late envelopes are unequal by an amount that is proportional to the amount of code phase error between the replica and the incoming signal (within the limits of the correlation interval). The code discriminator senses the amount of error in the replica code and the direction (early or late) from the difference in the amplitudes of the early

and late envelopes. This error is filtered and then applied to the code loop NCO, where the output code shift is increased or decreased as necessary to correct the replica code generator phase with respect to the incoming SV signal code phase.

5.2.3.3. Loop filter characteristics

| Loop Order | Noise Bandwidth B_n (Hz) | Typical Filter Values |
|------------|--|--|
| First | $\frac{\omega_o}{4}$ | ω_o $B_n = 0.25\omega_o$ |
| Second | $\frac{\omega(1+a_2^2)}{4a_2}$ | ω_o^2 $a_2\omega_o = 1.414\omega_o$ $B_n = 0.53\omega_o$ |
| Third | $\frac{\omega(a_3b_3^2+a_3^2-b_3)}{4(a_3b_3-1)}$ | ω_o^3 $a_3\omega_o^2 = 1.1\omega_o^2$ $b_3\omega_o = 2.4\omega_o$ $B_n = 0.7845\omega_o$ |

Table 5.4: Loop order filters

The values for the second-order coefficient a_2 and third-order coefficients a_3 and b_3 can be determined from Table 3. These coefficients are the same for FLL, PLL, or DLL applications if the loop order and the noise bandwidth, B_n , are the same. Note that the FLL coefficient insertion point into the filter is one integrator back from the PLL and DLL insertion points. This is because the FLL error is in units of hertz (change in range per unit of time).

5.3. Demodulation

Demodulation is the process of extracting the original information or base-band signal from a modulated carrier signal. The purpose of demodulation is to retrieve the modulating signal, which could be analog or digital data, audio, video, or other forms of information. Demodulation is essential in various communication systems such as radio, television, cellular networks, and wireless data transmission.

After the acquisition and tracking has been performed, the received data is mapped back using BPSK demodulation, mapping -1 to binary 1 and $+1$ to binary 0.

5.4. Decoding

Demodulated data is deinterleaved and sent to Channel decoding module for further processing. The deinterleaving process involves reversing the interleaving algorithm used during transmission. By applying the inverse operation, the interleaved data are rearranged back into their original order. Channel decoding involves the process of error correction and retrieval of the original data transmitted over the satellite link. The channel decoding scheme used in NavIC is based on a convolutional coding technique known as Rate $1/2$ Convolutional Code with Viterbi decoding.

5.4.1. Process

The high-level description of the channel decoding process in NavIC is shown in figure 5.5

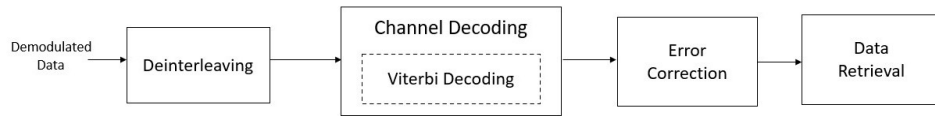


Figure 5.5: The Block Level Architecture for Channel decoding

5.4.2. Convolutional Code Representation

The convolutional code is represented as a state diagram or Trellis, where each state represents a unique history of the encoded bits. The Trellis consists of nodes and branches. Nodes correspond to states, and branches represent transitions between states. Each branch is labeled with the input bit and the encoded output bits associated with the transition.

5.4.2.1. Branch Metrics

At each time step, the Viterbi algorithm calculates branch metrics, which quantify the similarity between the received signal and the expected signal for each branch. The branch metric is typically based on a distance measure, such as Hamming distance or Euclidean distance, between the received signal and the expected signal. Let's denote the received signal at time step t as $r(t)$ and the expected signal for a particular branch as $c(t)$. The branch metric

$B(t)$ for that branch at time step t is computed as the distance between $r(t)$ and $c(t)$.

5.4.2.2. Path Metrics

The Viterbi algorithm computes a path metric for each state at each time step, which represents the accumulated likelihood of reaching that state along a particular path. The path metric is typically computed as the minimum (or maximum, depending on the metric used) of the sum of the previous path metric and the branch metric. Let's denote the path metric for state i at time step t as $P(i, t)$. The path metric for state i at time step t is computed as:

$$P(i, t) = \min_j P(j, t-1) + B(t), \text{ where } j \text{ is the previous state connected to state } i.$$

5.4.2.3. Survivor Paths

Along with the path metrics, the Viterbi algorithm keeps track of survivor paths, which represent the most likely paths leading to each state at each time step. The survivor paths are determined based on the branch with the smallest (or largest, depending on the metric used) branch metric leading to each state. The survivor paths help in traceback, as they indicate the most likely sequence of states leading to the current state.

5.4.2.4. Traceback

Once the decoding reaches the end of the received signal, a traceback process is performed to determine the final decoded sequence. Starting from the state with the highest path metric at the last time step, the algorithm traces back through the trellis by following the survivor paths. The traceback process continues until reaching the starting state at the first time step, yielding the decoded sequence of transmitted bits.

5.4.3. Decoding Output

The traceback process generates the final decoded output, which should ideally match the original transmitted data. The decoded output undergoes error correction, such as using error-correcting codes like Reed-Solomon, to further enhance the reliability of the decoded sequence.

The Viterbi algorithm is an iterative process that calculates and updates the path metrics and survivor paths at each time step. It efficiently explores all possible paths through the trellis and selects the most likely path. This results in the recovery of the transmitted data even in the presence of noise and errors.

5.4.4. Example

In the figure 5.6,

Transmitter side:

Left most 00, 01, 10, 11 - are the state s_0 , s_1 , s_2 and s_3 at time t . a/bb

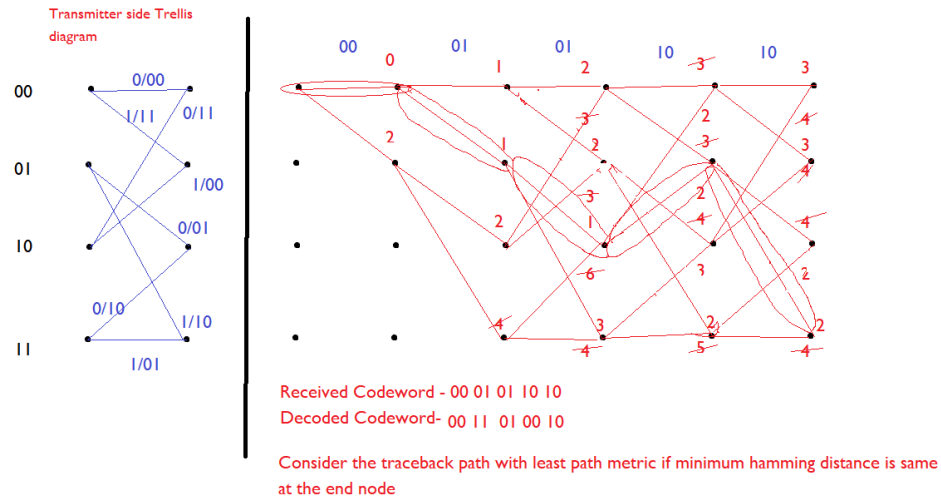


Figure 5.6: Trellis flow for Viterbi algorithm

means, for input a , output is bb for a given state transition.

Receiver side:

Assume the bits at top are received codewords - **00 01 01 10 10**. The codewords are compared with the possible transition states from the input diagram, thereby calculating hamming distance between received and possible outputs as per Trellis diagram. For example, for codeword 00, state is 00 and two possible paths are drawn in red. Hamming distance is calculated between received codeword 00 and possible outputs - 00, 11.

Similarly in the next step, for codeword 01, possible paths are from state 00 and state 01. Hence, hamming distance is calculated for all possible paths. When a node has 2 or more inputs, the least hamming distance is chosen. Branch metric is the minimum hamming distance value for a given path. Path metric is the sum of previously calculated path metric and current

branch metric. At the end, if the path metric value is equal for 2 different traceback paths, they are chosen with equal probability.

The process continues till the final codeword 10 is examined. Finally, a path with the least values of path metric is chosen. In this case the path from end to start is marked in the figure 5.6. The decoded codeword is determined as **00 11 01 00 10**.

The functions for acquisition and tracking are present in the below code

```
codes/demodulation/demodulation.py
```

The functions for decoding are present in the below code

```
codes/decoder/decode.py
```

The tracking results are generated using the code below and the plot is shown in figure 6.1.

Code

```
code/e2e_sim/main_ipynb
```

Chapter 6

Results

6.1. Acquisition

Acquisition results for PRN ID 5

Status:True Doppler:3500 Delay/Code—Delay:300/30.0

Acquisition results for PRN ID 7

Status:True Doppler:2500 Delay/Code—Delay:587/58.7

Acquisition results for PRN ID 3

Status:True Doppler:1500 Delay/Code—Delay:426/42.6

Acquisition results for PRN ID 1

Status:True Doppler:2500 Delay/Code—Delay:313/31.3

6.2. Tracking and Decoding

Result

Tracking and decoding output for PRN ID:5

Transmitted Bits:

```
[0. 1. 0. 1. 0. 0. 0. 1. 0. 1. 1. 0. 0. 0. 1. 1. 1. 0. 0. 1. 1. 1. 1. 0. 1. 0. 1. 1. 0.
 1. 0. 0. 1. 0. 0. 0. 1. 0. 1. 1. 1. 0. 1. 1. 0. 0. 1. 0. 0. 0.]
```

Received bits:

```
[1. 1. 0. 1. 0. 1. 1. 1. 0. 1. 0. 0. 1. 1. 1. 0. 0. 0. 1. 1. 0. 0. 0. 0. 1. 0. 0.
 1. 0. 1. 1. 0. 1. 1. 1. 0. 1. 0. 0. 0. 1. 0. 0. 1. 1. 0. 1. 1.]
```

Received bits inverted:

```
[0. 0. 1. 0. 1. 0. 0. 0. 1. 0. 1. 1. 0. 0. 0. 1. 1. 1. 0. 0. 1. 1. 1. 1. 0. 1. 1.
 0. 1. 0. 0. 1. 0. 0. 0. 1. 0. 1. 1. 1. 0. 1. 1. 0. 0. 1. 0. 0.]
```

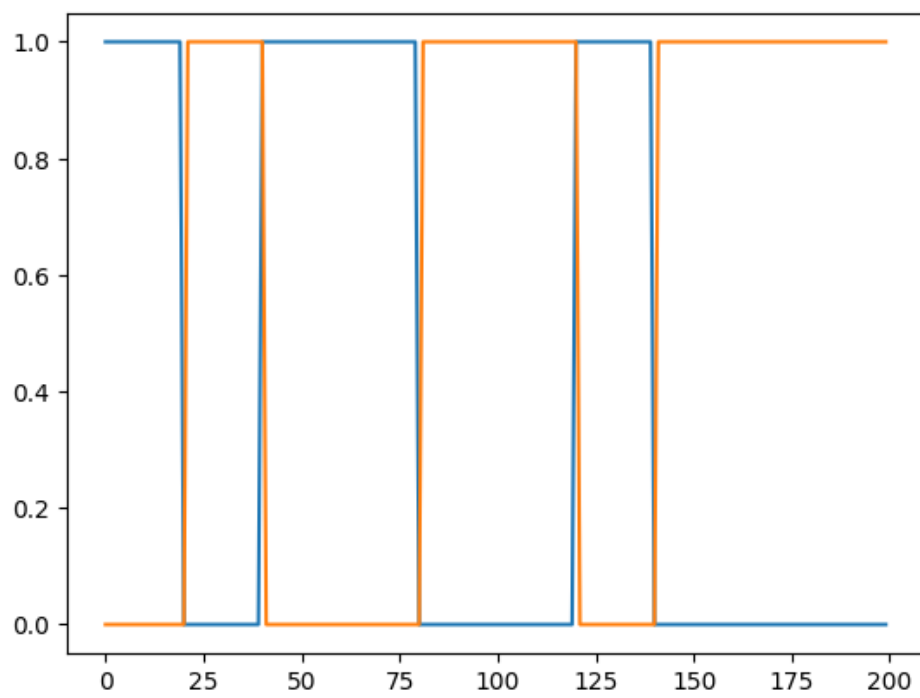


Figure 6.1: Tracking result plot

Appendix A

References

1. https://www.isro.gov.in/media_isro/pdf/Publications/Vispdf/Pdf2017/1a_messgingicd_receiver_incois_approved_ver_1.2.pdf
2. <https://gnss-sdr.org/docs/sp-blocks/acquisition/>
3. <https://gnss-sdr.org/docs/sp-blocks/tracking/>
4. Elliott D. Kaplan and Christopher J. Hegarty, Understanding GPS Principles and Applications, 3rd edition

